Photonics Integrations Enabling High-end Applications of InP in Optical Data Transmissions

Jiaming Zhang*, Newton Frateschi**, Ram Jambunathan, Wonjin Choi, and Aaron E. Bond

Apogee Photonics, Inc., Snowdrift Road, Suite 100, Allentown, PA USA 18106-9352
** Instituto de Física "Gleb Wataghin", Universidade Estadual de Campinas,
UNICAMP 13083-970, Campinas, São Paulo, Brazil
* jiaming.zhang@apogeephotonics.com; phone 1-610-289-5040; fax 1-610-289-5050; apogeephotonics.com

ABSTRACT

We present here results from a uniquely designed InP modulator chip combined with advanced packaging concepts, which enables high-end applications in optical data communications. An electroabsorption (EA) modulator, with a strained InGaAsP or InGaAlAs multiple quantum well structure, is monolithically integrated with a semiconductor optical amplifier. This design offers broad wavelength tunability while maintaining high extinction ratio, high optical output power, and high dispersion tolerance. The amplified EA modulator chip is co-packaged with a distributed feed back (DFB) laser ensuring separate optimization of the laser and modulator sections. The optical isolator, placed between the laser and modulator, completely eliminates adiabatic chirp. This Telcordia-qualified laser integrated modulator platform enables superior performance previously not thought possible for InP absorption based modulators. 11dB of dynamic extinction ratio, 5dBm of modulated output power, and ±1200ps/nm or +1600ps/nm dispersion tolerance can be simultaneously achieved in un-amplified 10Gb/s data transmission. Full C-band tunability using a single device is also demonstrated with the LIM module. Extensive simulations and transmission system evaluations shows that with the controllable chirp, the cost-effective LIM performs as well as a Mach-Zehnder modulator in dispersion managed and amplified long-haul WDM systems. Lastly, the first uncooled 10Gb/s long-reach operation at 1550nm was demonstrated with LIM packages. Using a simple control algorithm, a constant modulated output power of 1dBm with less than 1dB dispersion penalty over 1600ps/nm single mode fiber is achieved in an 80 degrees environmental temperature range without any module temperature control. Utilizing the Al-based material system, also allows a reduced variation of the extinction ratio.

Keywords: InGaAsP, InGaAlAs, Electroabsorption Modulator, Tunability, Uncooled, Data Transmission

1. INTRODUCTION

InP materials have been widely used in optoelectronic systems for many years. This is because InP is the only material which can generate, amplify, modulate, and receive light at wavelengths around 1550nm. In 2.5Gb/s transmission systems, electroabsorption modulated lasers (EML's) are deployed throughout many long haul systems as wavelength division multiplexed (WDM) transmitters. In applications where the bit rate is higher than 2.5Gb/s and the reach is longer than 40km the $LiNbO_3$ MZM is currently the preferred solution, especially in long-haul WDM transmission systems. $LiNbO_3$ MZM's have well controlled chirp, high extinction ratio, and low insertion loss. However, these well-controlled parameters come with the disadvantage of high drive voltage, large size, and high cost. The InP electroabsorption modulator (EAM) has traditionally been used in monolithically integrated structures with a DFB laser. EML's are attractive owing to their low drive voltage, small form factor, and low cost. However, EML's do not have the optical output power, extinction ratio, or chirp control to be widely used in 10Gb/s systems and longer than 80km in length. The integrated nature of these devices limits their transmission capabilities, NOT the InP electroabsorption process. Recent breakthroughs in hybrid package integration and in EAM photonic technology has significantly improved the performance of the isolated-laser integrated modulator module (LIM) over traditional EML's. In addition, the monolithic integration of a small optical amplifier with the EAM (EAMP) offers broad wavelength tunability while maintaining high extinction ratio, high optical output power, and small chirp. This type of transmitter made many high-end applications possible with InP materials. In

this paper we will present the performances of the LIM devices in 10Gb/s long-reach, and dispersion and power managed long-haul transmission systems. Full C-band tunable transmitter and long-reach uncooled operation of the LIM devices are also demonstrated.

2. ELECTROABSORPTION MODULATORS

Electroabsorption modulators (EAM) are based on the electro-absorption effect, which is defined as the change of light absorption in the presence of an electric field. The effects, known as Franz-Keldysh effect in bulk materials and the Quantum Confined Stark Effect (QCSE) in quantum well materials, result in absorption of photons with energies smaller than the bandgap with the application of an electrical field. This phenomenon can be used to convert electrical modulation to optical modulation. The quantum confined Stark effect is much stronger than the Franz-Keldysh effect and therefore results in much higher modulation efficiency. For this reason, most EAM's used in high speed systems are based on a multiple quantum well (MQW) structure [1].

2.1 InP-Based EAM

The electrical and optical properties of InP enable a large number of functions to be realized in one material system. The most obvious advantage of using an InP EAM is that the device can be made relatively small. The band gap energy of InP-based materials is close to the photon energies at wavelengths used in optical communications; so electro-optic and electroabsorption effects can introduced at low voltages and over small dimensions. In an InP-based EA modulator, large amount of light absorption can be achieved with about 2.5 V in about 200 μm.
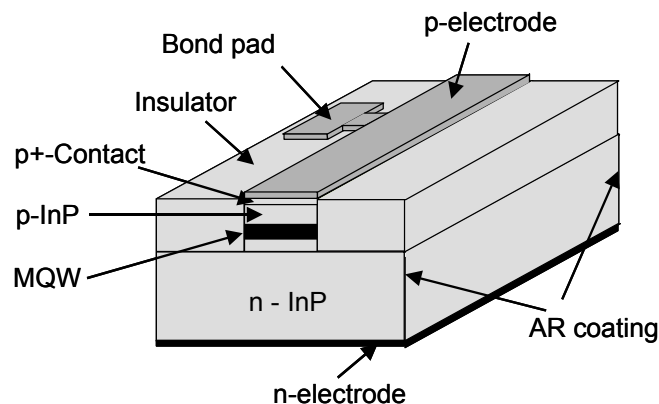

Figure 1: Schematic of an InP-based, MQW EA waveguide modulator

The conventional technique of applying a transverse bias across a MQW is to apply a reverse bias across a p-i-n diode, where the i-region includes a MQW structure. If the MQW is embedded in a waveguide structure, then the optical insertion loss of the waveguide, can be modulated by applying an electric field, and changes the absorption of the QW's through the effect described above. Figure 1 shows a schematic of an etched semiconductor waveguide modulator structure, in which light is transmitted horizontally through the structure. The typical thickness of the i-region is in the 0.1-0.5μm range, therefore it is possible to apply very strong electric fields with a few volts of reverse bias. Typical material systems used for making QW EA modulators include InGaAsP and InGaAlAs.

2.2 Electroabsorption Modulated Lasers (EML)

EML devices typical have the distributed feedback (DFB) laser and the EAM monolithically integrated into a single InP die [1]. The integration nature of the DFB laser and the modulator dramatically reduces the size of the transmitter and simplifies the packaging process. This kind of devices has been used extensively in metro

communication and long-haul systems at low data rates for many years. Unfortunately combining DFB and modulator sections into a single chip inherently introduces both optical and electrical crosstalks between the two sections. These crosstalks induce instabilities of the laser operation and frequency modulation of the DFB section. The modulated RF signal which drives the modulator section can take various paths to feed back to the DFB laser section. A slight electrical modulation of the DFB can cause laser wavelength modulation, broadening of laser linewidth, and on-state chirp of the modulator. Light reflections back to the DFB can cause similar problems. A schematic representation of the feedback experienced in an EML laser is shown in figure 2. The DC (adiabatic) chirp, defined as the optical frequency change of the transmitter between on- and off-states, limits the ability to transmit signals over long distances in dispersive fiber [1]. 10Gb/s integrated laser modulators are limited to 40-60km for most applications owing to this DC chirp limitation.
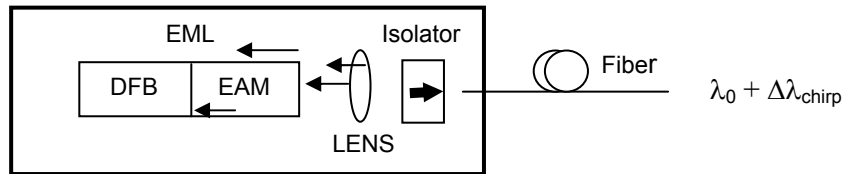

Figure 2: Schematic representation of the optical feedback caused by reflections from the facet of the EAM and facet of lens, and by scattering. This optical feedback introduces adiabatic chirp.

2.3 Laser Integrated Modulators (LIM)

The limitation of the EML is a direct result of both a non-ideal placement of the isolator and the electrical crosstalk between the physically adjacent laser and modulator sections. Ideally, the isolator should be positioned between the DFB and EAM sections. This prevents any reflections after the DFB from feeding back into the DFB and inducing an adiabatic chirp component to the signal. A schematic representation of the isolator being placed in between the laser and the EAM is shown in Figure 3. This architecture at Apogee is called the LIM (Laser Integrated Modulator) module. Physical separation of the DFB and the modulator sections, which breaks the paths of the possible electrical cross talk, and placing the optical isolator between the two elements enables the LIM platform performance to be suitable for many of the high-end applications previously not thought possible for InP modulators.
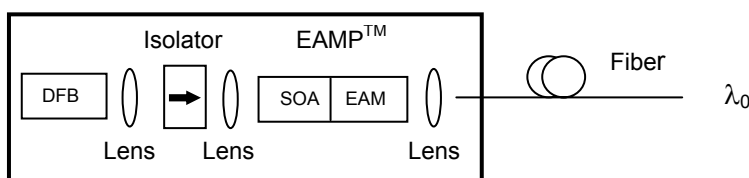

Figure 3: Schematic representation of a LIM where the isolator is placed between the EAM and the laser section. The isolator prevents feedback into the DFB and the result is that the device has zero adiabatic chirp.

An example of the elimination of the DC chirp component is shown in Figure 4. Figure 4a details the chirp as a function of time for a conventional EML structure. The thin lines represent the optical power out of the module as a function of time. The thick curves are the frequency deviations (chirp) as a function of time. Significant adiabatic chirp between the on- and off-states can be observed. This adiabatic chirp changes both in amplitude and sign as a function of the EA offset bias voltage. Due to the random nature of the phase of a cleaved facet and the variation of the chirp under varying bias or temperature conditions, the frequency chirp, which directly limits the transmission performance of the transmitter, becomes very hard to control. As one can see in Figure 4b, the LIM architecture introduces zero adiabatic chirp under all bias conditions. This is enabled through the use of the optical isolator and physical separation of the DFB and modulator sections. One can also see that more negative transient chirp can be achieved with increased EA offset bias. This type of chirp waveform is what is required to achieve high

transmission performance in a 10Gb/s link with fiber length of 100km. The effective chirp parameter, alpha, can be up to -0.7 in the most stringent applications.
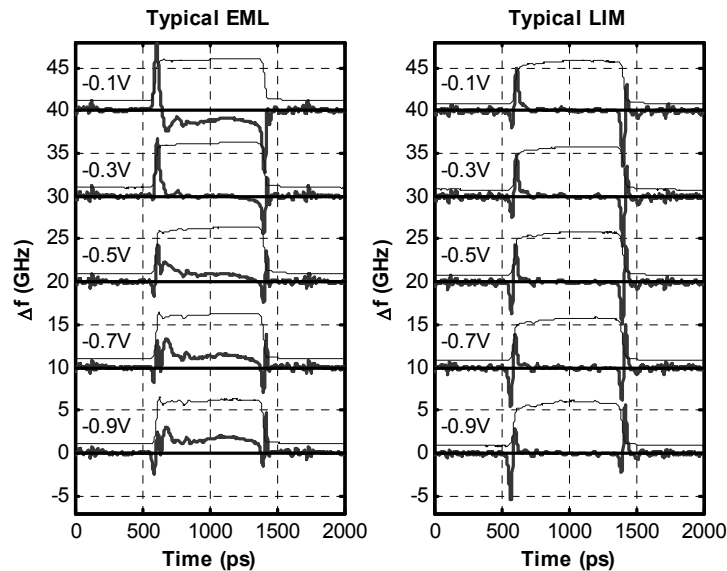

Figure 4: Typical EML power (thin lines) and chirp (thick lines) profile vs. time (a), and the LIM power (thin lines) and chirp (thick lines) profile vs. time (b). The placement of the isolator in-between the DFB and EAM section eliminates adiabatic chirp in the center of the pulse.

2.4 Amplified EAM (EAMP)

As shown in Figure 3, the amplified EAM (EAMP) has a semiconductor optical amplifier (SOA) monolithically integrated with the EAM section. Employing an integrated SOA allows the device to work over a wide wavelength tuning range without losing optical output power and chirp performance. The power amplification of the SOA makes it possible for the DFB to operate at low bias currents allowing excellent reliability of the LIM module. The SOA also allows for additional functionality, such as variable optical attenuation (VOA) and beam blanking during wavelength switching in WDM systems.

The multiple-quantum well structures for the EAM and SOA are grown monolithically by low-pressure metal-organic chemical vapor deposition. To enable longer wavelength operation, the SOA is grown with enhanced deposition rate using selective area growth (SAG). The epitaxial structure for the InGaAlAs EAMP also consists of a separated confinement layer design with an active region employing compressively strained InGaAsP and InGaAlAs quantum wells with tensile strain compensating barriers. A ridge waveguide is formed using a standard etching technology. After the waveguide formation, the device is planarized with polyimide to reduce the metal pad capacitance and standard p and n contacts are deposited by electron beam deposition. Antireflection coatings are deposited on both facets after cleaving. Further details of the MQW structures and the device processes can be found in [2] and [3].

3. LIM PERFORMANCES IN SYSTEM APPLICATIONS

3.1 10Gb/s TDM/WDM Long Reach Applications

In 10Gb/s TDM/WDM links of distances greater than 100km, cumulative dispersion of greater than 1600ps/nm, and where dispersion compensating fiber is not available, the modulator is put to the ultimate test. The high output power of the transmitter module, over +5dBm, is also needed for the power budget in long reach systems with

moderate receiver sensitivity. Due to the ultimate requirements of the device, this type of transmission distance and output power has traditionally been dominated by the LiNbO$_3$ MZM owing to its ability to achieve negative chirp factors of -0.7 and very low insertion loss of the structure. By properly engineering the EAM section of the LIM product, the LIM can achieve 100km transmission with high output power and extinction ratio with relative ease. Unlike an EML, a complete elimination of the adiabatic chirp in LIM allows a slightly less stringent requirement of the transient chirp without much degradation of the transmitted signal from fiber dispersion. This enables the modulator to work at a broad range of wavelength detuning relative to the DFB laser wavelength. This allows an offering of a complete family of transmitters in a single platform with varied output power for different applications in long-reach data transmission.

A typical 10Gb/s launch eye diagram is shown in Figure 5a, and the corresponding BER vs. received power curve is shown in Figure 5b. The LIM platform enables one to independently optimize blocking structures, quantum wells, and doping profiles of the modulator independent of the laser section. This further enables high yield WDM grid channels owing to the fact that the laser can be found at the right ITU wavelength independent of the modulator.

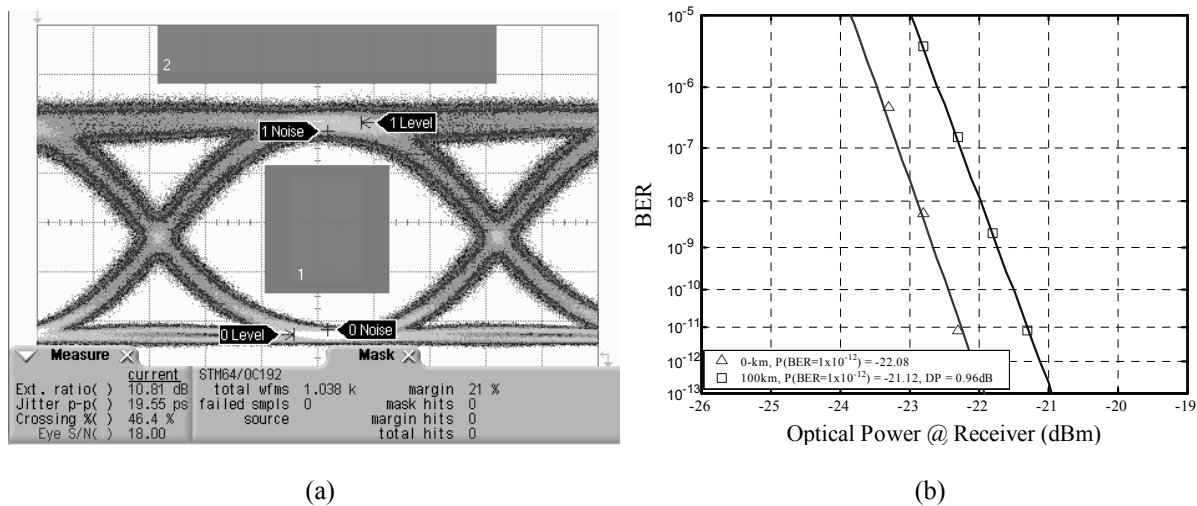

(a)   (b)

Figure 5: (a) Typical 10Gb/s launch eye diagram for a 1600ps/nm LIM product (SONET filter turned on, ER=10.8dB), modulated output power = 5.5dBm (b) Typical BER vs. received optical power for the 1600ps/nm LIM product, DP of less than 2dB is easily achievable. Separate optimization of the modulator from the laser enables superior transmission performance over an EML in a small form factor package.

3.2 Full C-Band Tunability

Widely tunable transmitters are an essential element of dense wavelength division multiplexed systems. Transmitters with full band coverage enables wavelength-agile functionality in addition to simplifying network provisioning and inventory reduction. Due to the transparent nature of the LiNbO$_3$ material over a broad wavelength range, today's full C-Band tunable 10Gb/s transmitter modules are designed with LiNbO$_3$ MZM. The EAMP chip provides wide wavelength tunability with high extinction ratio and output power. Using the hybrid integration concept shown in Figure 3, a full C-band tunable transmitter can be constructed with an industry standard tunable laser integrated with an EAMP chip in a small-form-factor with a footprint which is compatible with packages of standard hermetic butterfly modules. Small drive voltage down to 2.5Vpp range and a single thermoelectric cooler can be used for this type of module.

Figure 6 to 8 summarize the 10Gb/s modulation performance of such a module. At the top of Figure 6 are the composite optical spectra with the module operated under conditions at all the ITU channel wavelengths over C-band. SMSR, shown at the bottom of the figure, of greater than 35dB is achievable at all wavelengths. Figure 7 depicts the filtered optical eye diagrams for the module operating at the ITU channels 18, 40, and 61, which are at the wavelengths of 1563.03nm, 1545.32nm, and 1528.77nm, respectively. The power amplification functionality of the SOA allows modulated output power controllable to be constant at all channels. Figure 8(a) shows the RF

extinction ratios measured with the module operating at a constant output power of +1dBm across all channels. Extinction ratio greater than 11dB with SONET filter and greater than 12dB without the filter are achievable at all channels. Shown in Figure 8(b) are the power penalties measured with +1000 and -1000ps/nm fiber dispersion at each channel. The device was controlled to operate under equivalent-zero-chirp conditions where a symmetric dispersion tolerance is obtained. This is represented by the equal power penalties with positive and negative 1000ps/nm fiber dispersions. Under modified EA bias conditions, asymmetric dispersion tolerances of -400 and +1600ps/nm are achievable with the device. Modules covering all L-band spectra can also be constructed with L-band tunable lasers and an EAMP through the hybrid package integration using the same concept.
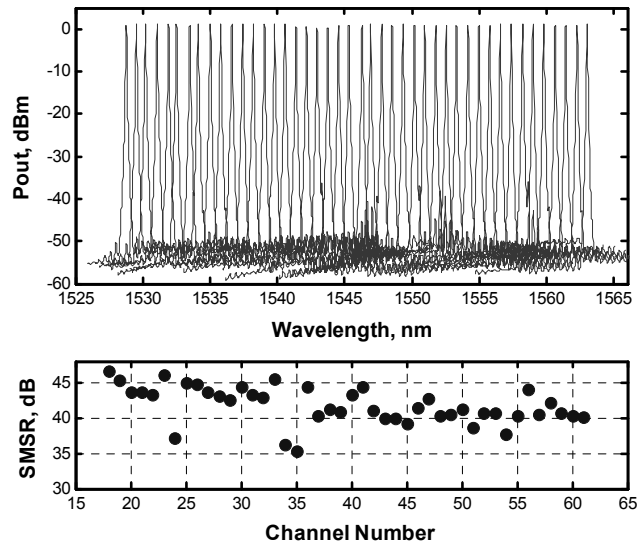

Figure 6: Top: laser spectra of all ITU channels across the C-band generated from a single tunable modulator module. Bottom: the corresponding side mode suppression ratio.
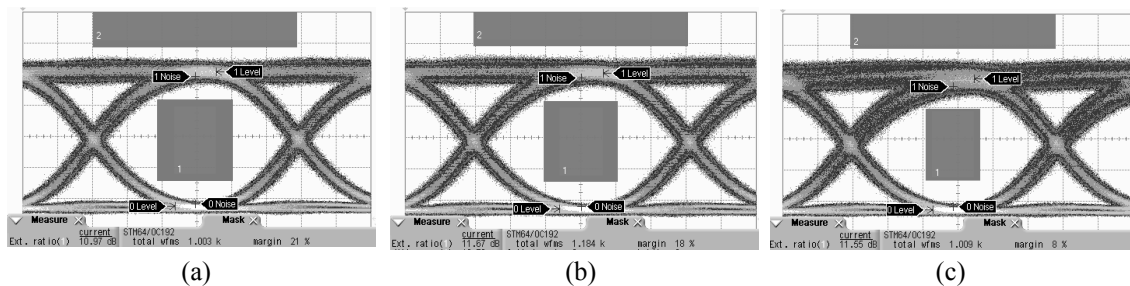

Figure 7: Optical eye diagrams at 10Gb/s with the tunable modulator module operating at ITU channels (a) 18, (b) 40, and (c) 61.

3.3 Dispersion and Power Managed Long-Haul Transmission

In this section, we demonstrate and explain why the LIM can perform equivalently well as a MZM in long-haul WDM systems by numerical simulations. We have previously presented error-free transmission of 10Gb/s optical data over 2000km single mode fiber using LIM devices [4]. The LIM transmitter model is constructed from experimental data for the simulations. We show that wide dispersion tolerance, comparable to a MZM, is observed both experimentally and from simulations using LIM transmitters. Simulation results with different configurations of long-haul WDM systems shows that nonlinear impairment can be eliminated through proper arrangement of fiber dispersion compensation. Using this type of transmitter in systems enables low channel penalty, which is tolerable to variations of the transmitter operating conditions.
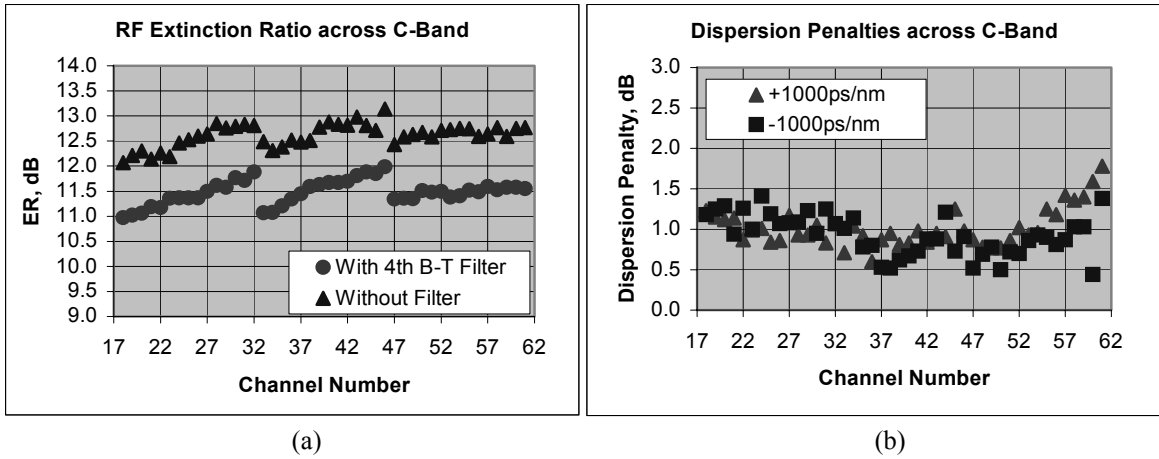
Figure 8: Link performances, at each ITU channel, of the full C-band integrated tunable transmitter module at 10Gb/s: (a) measured RF extinction ratio with and without the 4th order Bessel-Thomson filter; (b) power penalties with +1000ps/nm and -1000ps/nm fiber dispersions under zero-chirp operation conditions.

As discussed above, complete separation between the DFB laser and EAM in a LIM results in no crosstalk, both electrically and optically, between the two sections. Unlike an EML, this unique feature allows the EAM in the LIM to work purely as an external modulator, the same as a MZM. A simulation model for the transmitters was constructed with measured transfer functions, chirp alpha parameters, and RF responses. The accuracy of the model was verified by comparing the simulated dispersion tolerance to the experimental results. Figure 9(a) and (b), respectively, are the measured and simulated power penalty as a function of fiber dispersion for a zero-chirp MZM and a LIM operating at both zero-chirp and negative-chirp conditions. Simulations are in good agreement with the experimental results. When biased at the equivalent zero-chirp condition, symmetric dispersion tolerance of ±1400ps/nm can be achieved with a LIM, which is comparable to a chirp-free MZM. When biased at a negative chirp condition the LIM can tolerate as much as 1800ps/nm for a penalty less than 2dB.
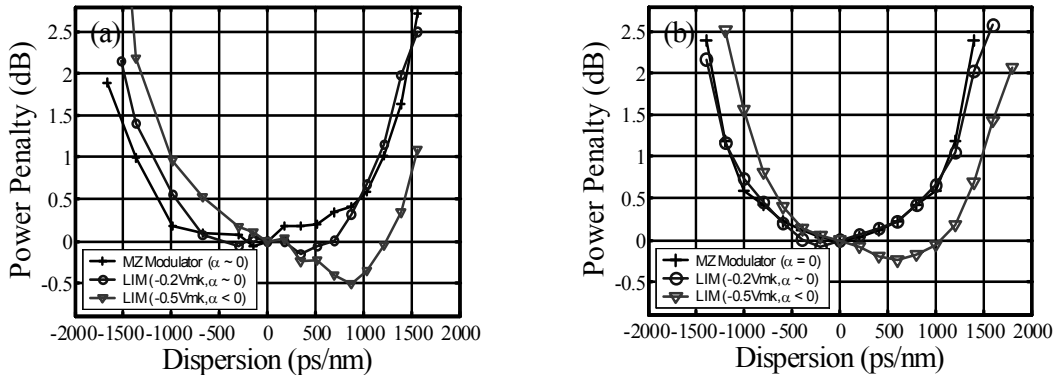

Figure 9: Experimental (a) and simulated (b) dispersion tolerances of the LIM and MZM

In a long-haul WDM system, OSNR degradation from amplifier noise accumulation requires increased channel power. On the other hand, fiber nonlinear effects excited at high launch powers will distort the transmitted signal. Owing to the interplay between fiber dispersion and nonlinear effects in direct-detection systems, fiber arrangement becomes critical for acceptable system performance in WDM links. Figure 10 shows an example of a dispersion managed and amplified WDM system, which can be optimized through simulations for balancing the system degradations from OSNR, dispersion, and nonlinear effects. 10Gb/s signals with 100GHz channel spacing are multiplexed and transmitted through a cascade of 90km non-zero dispersion shifted fiber (NZDSF, e.g. LEAF).

Attenuators after each of the optical amplifiers are used to adjust fiber launch power. Dispersion compensating fiber (DCF) with equal lengths is placed both in front of, and after, the link for pre- and post-compensations. Varying the length of the DCF fiber allows optimization of dispersion compensation. A simulation tool for nonlinear fiber transmission is used in the numerical modeling carried out in this work [5]. The tool utilizes a standard split-step-Fourier method to solve the nonlinear Schrödinger equation for describing the pulse propagation.
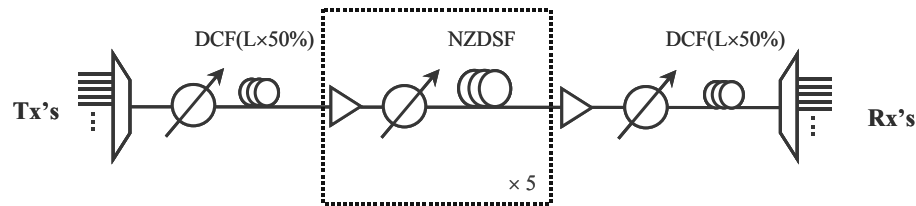

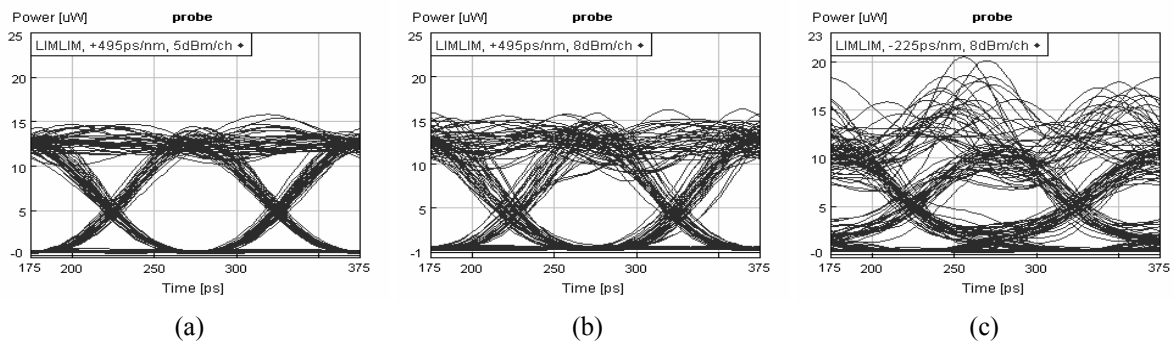Figure 10: Schematic of a WDM link of 5×90km non-zero dispersion shifted fiber with pre- and post-compensations.

(a)   (b)   (c)

Figure 11: Eye diagrams at the receiver side through 5×90km transmission: (a) total residual dispersion of +495ps/nm, fiber launch power of 5dBm/ch; (b) total residual dispersion of +495ps/nm, fiber launch power of 8dBm/ch; (c) total residual dispersion of -225ps/nm, fiber launch power of 8dBm/ch.
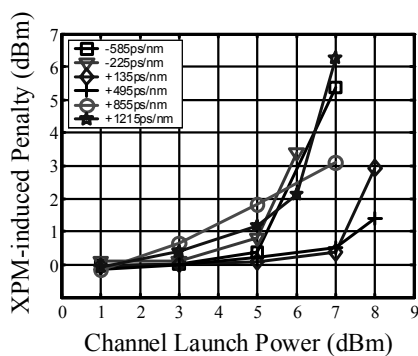

Figure 12: XPM-induced power penalty as a function of launch power with various residual dispersions in the link with LIM's under zero-chirp operation
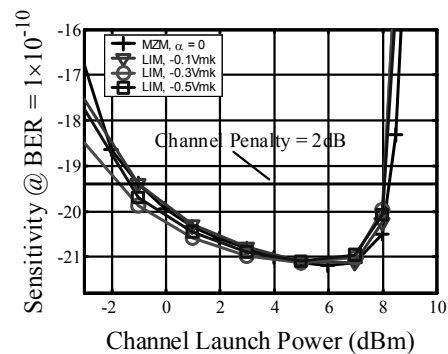
Figure 13: Receiver sensitivity as a function of optical launch power with optimal residual dispersion in the links with a chirpless MZM and LIM under various bias conditions.

Cross-phase modulation (XPM) and self-phase modulation (SPM) are two main sources of signal distortions at high launch powers in an amplified WDM system. Shown in Figure 11 are received eye diagrams simulated with the LIM operating under the condition with equivalent zero-chirp. Figure 11(a) is with a residual dispersion of +495ps/nm at a 5dBm channel power level. With an increase of the launch power by 3dB, nonlinear effects induce distortions, mainly owing to XPM, these distortions degrade the transmitted eye as shown in Figure 11(b). The received signal becomes more distorted, as shown in Figure 11(c), at the same launch power as in (b) but with unsuitable dispersion compensation. In the last case both SPM and XPM dominate the distortions. XPM suppression using a proper dispersion management is further demonstrated in figure 12 where the XPM-induced power penalty was simulated as a function of channel power with varied residual dispersions in the system. The XPM-induced power penalty can be obtained by taking out the sensitivity degradation from all other impairments in a single channel system [6]. It clearly shows that with certain amount of under-compensation in the positive dispersion system, XPM can be suppressed so the system can tolerate significantly higher launch power. The optimal residual dispersion is around +495ps/nm, which is equivalent to a 75% compensation ratio in the link shown in Figure 10. This optimal compensation ratio varies in different links. It is found that a 94% compensation ratio, i.e. a residual dispersion of +680ps/nm, provides the best performances for a link of 8×80km standard single mode fiber.

Figure 13 shows the receiver sensitivity as a function of channel power with optimal dispersion compensation in the system. Successful suppression of the nonlinear impairments allows a fiber launch power of 5dBm/ch where OSNR degradation can be minimized. A channel penalty of less than 0.5dB is achievable from the optimizations. This small channel penalty is equivalent to what can be achieved with a zero-chirp MZM with which the optimized receiver sensitivities are also shown in Figure 13. It is important to point out that the wide open dispersion tolerance is beneficial for such low channel penalty since this yields a negligible linear dispersion power penalty with a significant amount of residual dispersion in the system. We further examined the system performances as a function of the EA bias, combined bandwidth of transmitter and RF driver (in a region of 7 to 15GHz), and extinction ratio (from 10 to 14dB). While extinction ratio has an impact at low launch power as expected, the resultant variations in receiver sensitivity due to the transmitter parameter variations are within 0.5dB under the optimal conditions in the systems.

In a summary, nonlinear impairments can be suppressed with proper dispersion management using a LIM. Owing to its small transient chirp, large extinction ratio, and most importantly a complete elimination of adiabatic chirp; the LIM has a dispersion tolerance as wide as a zero-chirp MZM. This allows the LIM to perform as well as a MZM in dispersion managed and amplified long-haul WDM systems.

3.4   Uncooled Long Reach Data Transmission

Owing to tight restrictions in size, power, and price, uncooled operation of a laser transmitter is essential to designs of small-form factor 10Gb/s transceivers, such as XFP, X2, and XPAK. For 10Gb Ethernet and SONET/SDH applications at intermediate and long reaches, 1550nm transmitters are required. Because lasers and modulators at 1550nm are more temperature-sensitive than 1310nm lasers, and chirp performance needs to be more precisely controlled to tolerate fibre dispersion, uncooled operation of long reach 1550nm EAM-based devices has not been previously demonstrated. We have presented the first 1550nm laser integrated modulator module using the LIM platform that can be utilized for uncooled 10Gb/s long reach data transmission [7].

When a laser is heated up, laser threshold current increases and slope efficiency decreases. Also, the mismatch between modulator band gap shift (~0.5nm/°C) and laser emission wavelength change (~0.1nm/°C) with increased temperature induces a significant increase in light absorption. Both effects result in a reduction of output power of a modulator coupled to the laser. This becomes one of the most serious challenges for uncooled operation of a 1550nm transmitter. Using the EAMP design described above, Apogee has overcome these challenges. The power loss is compensated by the monolithically integrated SOA. Superior chirp characteristics and RF response performance of the EAMP chip allows an operation over the wide range of detuning between laser wavelength and modulator absorption edge. Figure 14-18 show some of the experimental results with a uncooled LIM package with the EAMP chip in the InGaAsP quantum well system.

Figure 14 are measured DC transfer curves of a typical uncooled LIM package at various temperatures. By proper choice of the detuning, high extinction ratio and output power can be achieved from 0 to 70°C. Figure 15 shows the characteristics of the uncooled LIM with the EA bias adjusted to achieve equivalent performance in the entire temperature range. A simple linear fit of these EA bias voltages, shown in Figure15(a), provides a simplified control algorithm for uncooled operation of the LIM package. In the experiments, a constant 2.5Vpp 10Gb/s signal is applied through a commercial RF driver to the device. Shown in Figure 15(b-e) are real-time simultaneously measured results of modulated output power (Pout), extinction ratio (ER, solid curve), eye crossing percentage (Cr), and 94km dispersion penalty (DP) with the LIM device under an active control while its temperature is adjusted from 0 to 70°C. Pout can be maintained at 1dBm in the entire temperature range. Because the device is controlled to be at the bias points where the modulator transfer and chirp performances are equivalent at each temperature, DP and Cr are almost independent of temperature.
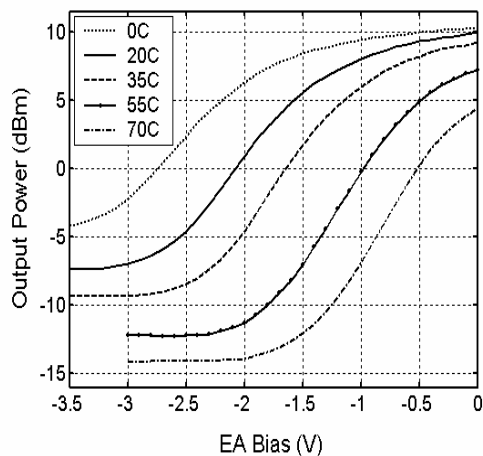

Figure 14. Light-voltage (LV) transfer curves of the uncooled LIM module at varied temperature from 0 to 70°C.
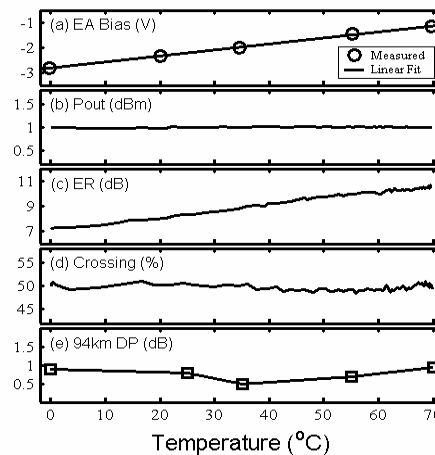

Figure 15. EAM bias voltages (a) and monitored performances (b-e) under an active control of the uncooled LIM module
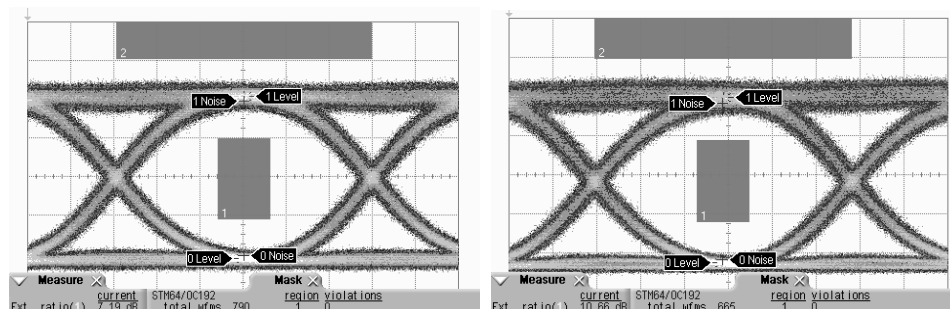

Figure 16. 10Gb/s optical eye diagrams at package case temperatures of 0°C (left) and 70°C (right). ER's measured with SONET filter are 7.2 and 10.7dB, respectively.

Typical filtered optical eye diagrams are shown in Figure 16 for package temperatures at 0 and 70°C, respectively. Wide-open eye with mask margins of greater than 20% are achievable over the entire temperature range. This is partially attributed to the high bandwidth (BW) of the LIM devices. Shown in Figure 17 are the small signal S21

response at 0 and 70°C, respectively. Slight reduction of the –3dB BW is observed at high temperatures. However even at 70 °C, this BW can be as high as 15GHz. This performance allows an uncooled operation of the LIM modules at OC-192 FEC rates without difficulties.

Shown in Figure 18 are BER waterfall curves, in a double log scale, measured with a 10Gb/s PRBS data stream of $2^{31}-1$ for back-to-back and with 94km SMF-28 fiber (1600ps/nm) at 0 and 70°C, respectively. As already shown in Figure 15(e), dispersion penalties, determined at BER=1×10^{-12}, are both around 1dB. The back-to-back receiver sensitivity is degraded at 0°C due to lower ER. However, the total power penalty for both ER and dispersion is below 2dB.
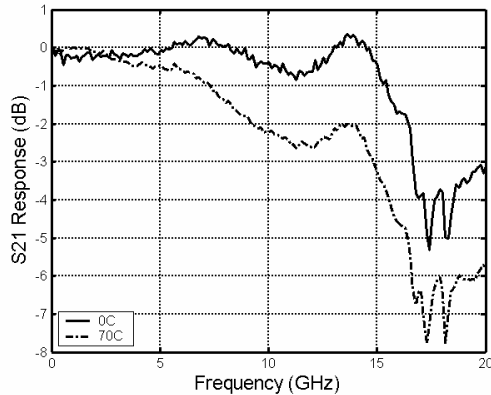

Figure 17. Normalized small signal S21 responses of an uncooled LIM packages at 0 and 70°C.
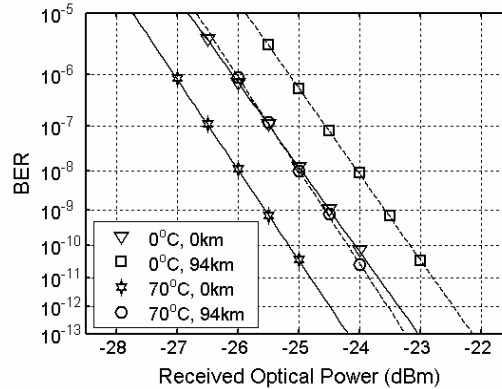

Figure 18. BER waterfall plots at back-to-back and with 94km single mode fiber (1600ps/nm) measured with an uncooled LIM module at 0 and 70°C.
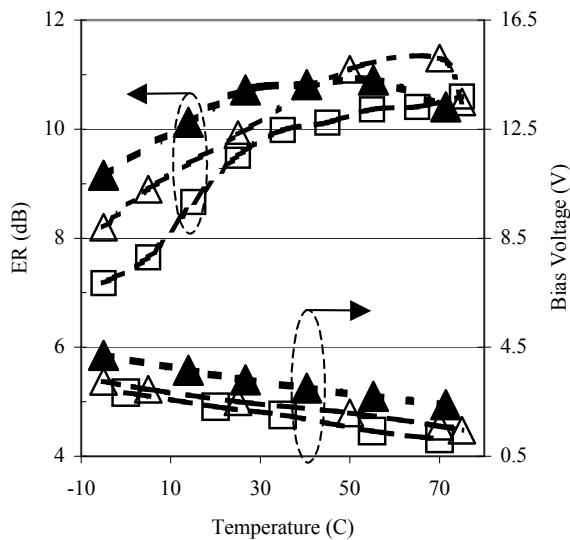

Figure 19. Transmission characteristics over temeprature. Left axis: filtered RF ER. Right axis: the absolute values of DC bias. Dispersion penalty is always 1 dB and output power 0 dBm. Module A (open squares): InGaAsP/InP; module B (solid triangles): low field InGaAlAs/InP; and module C (open triangles): high field InGaAlAs/InP.

While the InGaAsP QW system show excellent performance as described above, the RF extinction ratio varies 3.5dB from 0 to 70°C (see Figures 15 and 16). The 7.2dB ER at the lowest temperature doesn't meet the ITU IR2 and LR2 standard requirements. Improvements can be made with increased RF drive swing voltage at lower temperatures. However this approach relays on the availability of the 10Gb/s EML drivers on the market and it complicates the control algorithm and circuit designs. EAMP's with InGaAlAs QW system has been developed to improve the extinction ratio and its variation across temperature [8-9]. The higher conduction band discontinuity of the InGaAlAs/InP material system allows much greater oscillation strength. At low temperatures where high EA bias voltages are required to achieve suitable chirp, the enhanced oscillation strength becomes essential for maintaining enough electron-hole wave-function overlap, and thus high extinction ratio. The reduction of the ER variation with the InGaAlAs QW system can be found from the measured data shown in Figure 19 with three uncooled LIM modules using the InGaAsP (square) and InGaAlAs (filled and open triangles) QW material systems. All measurements were taken under the laser/SOA and EA bias conditions for constant output power of 0dBm and dispersion penalty of 1dB across the temperature range. Both InGaAlAs QW designs shown in the figure significantly improve the ER variation and bring the ER characteristics within the ITU IR2 specification. The low field design (solid triangles) has undoped graded region. This results in a low build-in field in the active region, and consequently, requires higher EA bias voltages, up to -4.2V at the lowest temperature. The second design, shown as open triangles in the figure, with reduced graded-layer thickness and increased doping concentration greatly enhance the built-in field and reduces the operation EA bias voltage down to -3.2V at the lowest temperature [9].

4. CONCLUSION

InP EAM modulators have traditionally been limited to metro distances of <60km owing to the disadvantage of trading off modulator performance with laser performance in an integrated EML structure. The monolithic integration of SOA and EAM and hybrid packaging integration in the LIM platform enables one to separately optimize the laser from the modulator and achieve performance on par with LiNbO$_3$ MZM in a smaller footprint, and lower cost to the system integrator. High performances in the LR and in the amplified and dispersion managed long-haul transmission systems are demonstrated. Full C-band tunability and uncooled operation of the LIM devices are also presented. With the recent progresses in the integration technologies, the InP modulator is expected to replace most existing LiNbO$_3$ applications.

5. REFERENCES

1. Kaminow, I.P., and Koch, T.L., *Optical Fiber Telecommunications IIIA*, San Diego CA: Academic Press, 1997
2. Choi, W., Bond, A.E., Kim, J., Zhang, J., Jambunathan, R., Foulk, H., O'Brien, S., Van Norman, J., Vandegrift, D.V., Wanamaker, C., Shakespeare, J., and Cao, H., "Low insertion loss and low dispersion penalty InGaAsP quantum well high speed electroabsorption modulators," *IEEE Journal of Lightwave Technologies*, vol. **20**, pp.2052-2056, 2002.
3. W. Choi, N. Frateschi, J. Zhang, H. Gebretsadik, R. Jambunathan, A. E. Bond, J. Van Norman, D. Vandegrift, and C. Wanamaker, 'Full C-band tunable high fiber output power electroabsorption modulator integrated with semiconductor optical amplifier', *Electronics Letters*, 2003, vol. **39**, pp. 1271, 2003.
4. L. Zhang and X. D. Cao, "Long haul transmission using electro-absorption modulators", *Technical Proceeding of NFOEC'2002*, paper **P447,** pp.1204, 2002
5. VPIsystems Inc., www.vpiphotonics.com.
6. V. Mikhailov, R. I. Killey, J. Prat, and P. Bayvel, "Limitation to WDM transmission distance due to cross-phase modulation induced spectral broadening in dispersion compensated standard fiber systems", IEEE Photon. Technol. Lett., **11**, 994-996 (1999).
7. J. Zhang, N. Frateschi, W. Choi, H. Gebretsadik, R. Jambunathan, and A. E. Bond, "A laser integrated modulator module for uncooled, 10Gbit/s 1550 nm long reach data transmission", *Electronics Letters*, vol. **39**, pp.1841-1842, 2003.

8. N.C. Frateschi, J. Zhang, W.J. Choi, H. Gebretsadik, R. Jambunathan, A.E. Bond, "High performance uncooled C-band, 10 Gb/s InGaAlAs MQW electro-absorption modulator integrated to Semiconductor Amplifier in Laser integrated modules", *Electronics Letters*, vol. 40, pp. 140-141, Jan. 2004.
9. N. C. Frateschi, J. Zhang, R. Jambunathan, W. J. Choi, C. Ebert, and A. E. Bond, "Long reach uncooled performance of 10 Gb/s Laser integrated modules with InGaAlAs/InP and InGaAsP/InP MQW electro-absorption modulators monolithically integrated with Semiconductor Amplifiers", *IEEE Photon. Technol. Lett.*, vol 17, pp1378-1380.